Field Theoretical Approach to Dynamics of Plastic Deformation and Fracture

S Yoshida

Field Theoretical Approach to Dynamics of Plastic Deformation and Fracture

S. Yoshida

Department of Chemistry and Physics, Southeastern Louisiana University
Hammond, LA 70402, USA

Abstract. Based on the field theoretical approach developed by physical mesomechanics and recent analysis on the associated gauge field, deformation of solid-state materials is formulated as a linear transformation of infinitesimal line elements in a deforming object. This formalism is capable of describing all stages of deformation including fracture on the same theoretical basis. The elastic and plastic stages are differentiated by whether the transformation is global or local. From the gauge invariance of the transformation and the least action principle applied to the gauge field, dynamics of plastic deformation is obtained being characterized as decaying, transverse wave behavior of the displacement field. Fracture is characterized as the final stage of deformation where the material becomes totally dissipative and the displacement wave decays completely. Optical interferometric experiment has been carried out to analyze in-plane displacement of a metal specimen under tensile loading. The result of analysis indicates that the plastic deformation and fracture criteria derived from the present formalism are able to reveal the transition from the elastic to plastic stage and predict the initiation of crack growth.

INTRODUCTION

Study on deformation and fracture of solid-state materials has a long history. Conventionally, however, different stages of deformation are treated with fundamentally different approaches. The elastic theory [1] is based on the well-known stress-strain tensor formalism, prevailing theories of plasticity [2] are mostly phenomenological, and fracture mechanics [3] is based on energy-balance or stress intensity approach. This situation makes difficult to apply these theories to analysis of transitional stages. In particular, the transition from developed deformation to fracture is hard to analyze, leading to a number of catastrophic accidents. More comprehensive approaches are essential for a major breakthrough in this field.

In this regard, the field theoretical approach developed by physical mesomechanics [4, 5] has great potential. Based on the principle of gauge invariance [6], this approach is capable of describing all stages of deformation on the same theoretical basis [5]. The principle of gauge invariance states that the Lagrangian is invariant under a certain continuous group of local transformations [7]. In the present context, the concept can be described as follows. When a material deforms elastically, a line element vector (the position vector connecting two nearby points in the material) transforms linearly. The mathematical representation of this transformation can be put

in the form of a matrix known as the distortion matrix whose elements are strain and rotations. Since the displacement is a linear function of the coordinates, all the distortion tensor matrix elements are constant. (They are first-order spatial derivatives of displacement). Equivalently, we can say that the transformation is identical at all points in the material, or the transformation is global. When the material enters the plastic regime, this global linearity is lost. However, if we focus on local regions of the material where the displacement is infinitesimal, we can still assume that the deformation is locally linear. The difference from the elastic case is that each of these local regions now transform differently from one another; the transformation is local or coordinate-dependent. Since the distortion matrix elements contain derivatives and they depend on the coordinates, it becomes necessary to replace the usual derivatives with covariant derivatives, i.e., to introduce a gauge (connection) field so that the Lagrangian is invariant [7]. The dynamics of plasticity is associated with this extension of the transformation being global to local, and can be described via the analysis of the gauge field. The application of least action principle to this gauge field yields a constitutive equation in plasticity. Note that this invariance is different from the invariance associated with frame indifference in continuum mechanics [8], which states that the constitutive relationship should be unaffected by rigid body motions the material may be undergoing.

Interestingly, from the field theoretical viewpoint, this dynamics is analogous to electrodynamics. The mesomechanical field equations can be put in the form of the Maxwell equations, and the decaying characteristic of a displacement wave in a plastically deforming material [9] is analogous to an electromagnetic wave travelling in a conductive medium. The similarity between the deformation dynamics and electrodynamics is not necessarily surprising, if we note that the electromagnetic field can be viewed as the gauge field to make quantum dynamics locally symmetric [7]. Noting this similarity with the electromagnetic field, the present author has investigated various aspects of the deformation field both theoretically and experimentally. Using an optical interferometric technique known as the electronic speckle pattern interferometry [10], we observed decaying transverse displacement waves [9]. Based on the analogy to electrodynamics, we have interpreted physical meaning of various physical mesomechanical observations, and have derived the constitutive equation in plasticity [11].

The aim of this paper is to outline the gist of this gauge theoretical formalism and present recent experiments as an example of engineering application of the theory. The present formalism is based on the original work done by Panin et al. [5], and recent addition and modification made by the present author.

FOMULATION

Deformation as a Linear Transformation

For simplicity, we discuss the formulation using in a two-dimensional model. The discussion can be extended to three dimensions based on a similar argument. Consider an infinitesimal line element vector $\vec{\eta}(x, y)$ connecting points P and Q in a

deforming material (Figure 1). Assume that the two points displace to P' and Q' in unit time. The resultant changes in vectors $\overrightarrow{OP}$ and $\overrightarrow{OQ}$ can be written as follows

$$\overrightarrow{OP'} = \overrightarrow{OP} + \vec{V}(x, y) \tag{1}$$

$$\overrightarrow{OQ'} = \overrightarrow{OQ} + \vec{V}(x + \eta^1, y + \eta^2), \tag{2}$$

where $\vec{V}$ is the displacement vector per unit time, and η^1 and η^2 are the x and y components of the line element vector.

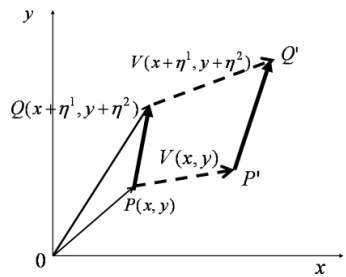

FIGURE 1. Change in infinitesimal line element vector in a deforming material.

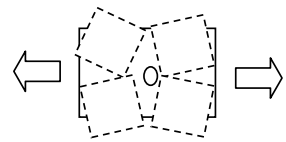

FIGURE 2. Schematic view of material rotations of four segments around a defect. Arrows represent applied forces.

We can view this change in the line element as the following linear transformation.

$$\begin{bmatrix} \eta'^1 \\ \eta'^2 \end{bmatrix} = \begin{bmatrix} \eta^1 \\ \eta^2 \end{bmatrix} + \begin{bmatrix} \frac{\partial u}{\partial x} & \frac{\partial u}{\partial y} \\ \frac{\partial v}{\partial x} & \frac{\partial v}{\partial y} \end{bmatrix} \begin{bmatrix} \eta^1 \\ \eta^2 \end{bmatrix} = (I + \beta) \begin{bmatrix} \eta^1 \\ \eta^2 \end{bmatrix} = U \begin{bmatrix} \eta^1 \\ \eta^2 \end{bmatrix}, \tag{3}$$

where u and v are the x and y components of $\vec{V}$, I is a unit matrix, and transformation matrix U and distortion matrix β are defined as below.

$$U = I + \beta \tag{4}$$

$$\beta = \begin{bmatrix} \frac{\partial u}{\partial x} & \frac{\partial u}{\partial y} \\ \frac{\partial v}{\partial x} & \frac{\partial v}{\partial y} \end{bmatrix}. \tag{5}$$

Considering all modes in the two-dimensional deformation and viewing them as forming a group, we can rewrite the distortion matrix in the following form.

$$\beta = \varepsilon_{xx}\begin{bmatrix}1 & 0\\ 0 & 0\end{bmatrix} + \varepsilon_{yy}\begin{bmatrix}0 & 0\\ 0 & 1\end{bmatrix} + \varepsilon_{xy}\begin{bmatrix}0 & 1\\ 1 & 0\end{bmatrix} + \omega_z\begin{bmatrix}0 & -1\\ 1 & 0\end{bmatrix} = \beta^a T_a . \qquad (6)$$

Here, distortion matrix parameters ε_{xx}, ε_{yy}, ε_{xy}, and ω_z represent the normal strains ($\varepsilon_{xx} = \partial u/\partial x, \varepsilon_{yy} = \partial v/\partial y$), shear strain [$\varepsilon_{xy} = 1/2(\partial v/\partial x + \partial u/\partial y)$] and rotation [$\omega_z = 1/2(\partial v/\partial x - \partial u/\partial y)$], respectively. The right-most hand side of eq. (6) indicates that the distortion matrix parameters can be viewed as group parameters (β^a), where the index a denotes the group elements and T_a the corresponding generators.

Gauge Invariance

When the deformation is elastic, the distortion matrix parameters are all constant (being linear, the first-order derivatives appearing in ε_{xx}, etc. are constant), hence the transformation U is coordinate-independent (global). On the other hand, when the deformation is plastic, these parameters become coordinate-dependent (local). We can intuitively understand this situation by considering a defect generated in a deforming material (Figure 2). Naturally, the four blocks around the defect have the freedom in rotating differently; rotation becomes coordinate dependent.

When the transformation U is local, the derivative of the line element vector after transformation, $\partial/\partial x_\mu(U\vec{\eta})$, is not the same as the transformation of the derivative of $\vec{\eta}$; i.e., $\partial/\partial x_\mu(U\vec{\eta}) = (\partial U/\partial x_\mu)\vec{\eta} + U(\partial\vec{\eta}/\partial x_\mu) \neq U(\partial\vec{\eta}/\partial x_\mu)$. In other words, the derivative does not transform in the same fashion as the vector itself, indicating that the Lagrangian is not invariant under the transformation U . If this is the case, U is physically meaningless. Thus, it becomes necessary to replace the usual derivative by a covariant derivative $D_\mu = \partial/\partial x_\mu - \Gamma_\mu$. Here x_μ denotes t , x , y , or z as the suffix varies $\mu = 0,1,2,3$, and Γ_μ is the gauge associated with the derivative along x_μ . Replacing the usual derivatives with the covariant derivatives, we can derive the transformation that Γ_μ must obey so that the derivatives transform in the same fashion as the vector. The transformation of the covariant derivative of $\vec{\eta}$ is now given as

$$U(D_\mu\vec{\eta}) = U(\partial\vec{\eta}/\partial x_\mu) - U(\Gamma_\mu\vec{\eta}) , \qquad (7)$$

whereas the covariant derivative of the transformed vector is

$$D_\mu(U\vec{\eta}) = (\partial U/\partial x_\mu)\vec{\eta} + U(\partial\vec{\eta}/\partial x_\mu) - \Gamma_\mu'(U\vec{\eta}) . \qquad (8)$$

Here Γ_μ' denotes the gauge associated with the covariant derivatives after the transformation. Equating Eqs. (7) and (8) and using Eq. (4), we obtain $-(I+\beta)\Gamma_\mu\vec{\eta} = (\partial\beta/\partial x_\mu)\vec{\eta} - \Gamma'_\mu(I+\beta)\vec{\eta}$, which relates Γ_μ' and Γ_μ as below

$$\Gamma_\mu'(I+\beta) = \partial\beta/\partial x_\mu + (I+\beta)\Gamma_\mu . \tag{9}$$

Dropping the second-order term, we obtain that $(I-\beta)(I+\beta) = I+\beta-\beta = I$, and hence $(I+\beta)^{-1} = (I-\beta)$. By multiplying this expression of $(I+\beta)^{-1}$ from the right and dropping the second-order terms, Eq. (9) becomes

$$\Gamma_\mu' = \Gamma_\mu + \partial\beta/\partial x_\mu + [\beta, \Gamma_\mu] . \tag{10}$$

Expressing β and Γ_μ with group elements as $\beta = \beta^a T_a$ and $\Gamma_\mu = \Gamma_\mu{}^a T_a$, and using the structure constant f_{bc}^a, we can rewrite the last term on the right-hand side of Eq. (10) as $[\beta, \Gamma_\mu] = [\beta^b T_b, \Gamma_\mu^c T_c] = \beta^b \Gamma_\mu^c [T_b, T_c] = f_{bc}^a \beta^b \Gamma_\mu^c T_a$, and the entire equation as

$$\Gamma_\mu{}'^a = \Gamma^a{}_\mu + \partial\beta^a/\partial x_\mu + f_{bc}^a \beta^b \Gamma_\mu{}^c . \tag{11}$$

Field Equations

Defining vector potential $A^\mu = l^2 \Gamma^\mu$ [12] and stress tensor $F^{a\mu\nu}$ as

$$F^{a\mu\nu} = \partial^\mu A^{a\nu} - \partial^\nu A^{a\mu} + f_{bc}^a A^{b\mu} A^{c\nu} , \tag{12}$$

where l is the characteristic length of the local area corresponding to the locally defined transformation U, we find that Lagrangian L in the following form is invariant under the transformation (11).

$$L = -\frac{1}{4} F_{\mu\nu} F^{\mu\nu} + g^{ij} D_\mu \eta_i^\alpha D_\nu \eta_j^\beta C_{\alpha\beta}^{\mu\nu} , \tag{13}$$

where g^{ij} is the metric tensor and $C_{\alpha\beta}^{\mu\nu}$ is the dimensionless elastic tensor of the material when all indices are spatial ($\alpha, \beta, \mu, \nu = 1,2,3$). When the indices are spatio-temporal, $C_{\alpha\beta}^{0\nu} = -\delta_{\alpha\beta}\delta^{0\nu}$, $C_{0\beta}^{\mu\nu} = -\delta_{0\beta}\delta^{\mu\nu}$, $C_{0\beta}^{0\nu} = \delta^{0\nu}\delta_{0\beta}$ [5]. Applying the least action principle to the above defined Lagrangian

$$\partial_\nu \left(\frac{\partial L}{\partial(\partial_\nu A_\mu)} \right) - \frac{\partial L}{\partial A_\mu} = 0 , \tag{14}$$

we obtain the following field equations:

$$F_{,\nu}{}^{a\mu\nu} = -g^{ij} T_i^{ak} \eta_k^\alpha D_\nu \eta_j^\beta C_{\alpha\beta}^{\mu\nu} / l^2 . \tag{15}$$

Substituting Eq. (12), we can put Eq. (15) as below:

$$\partial_\nu(\partial^\nu A^{a\mu}) - \partial^\mu(\partial_\nu A^{a\nu}) - f^a_{bc}A^b_\nu F^{c\mu\nu} = -g^{ij}T_i^{ak}\eta_k^\alpha D_\nu\eta_j^\beta C^{\mu\nu}_{\alpha\beta}/l^2. \tag{16}$$

Using the vector form, we can further rewrite Eq. (16) as below:

$$\nabla\cdot S^a - f^a_{bc}(A^b\cdot S^c) = g^{ij}T_i^{ak}\eta_k^\alpha\dot{\eta}_j^\beta/l^2 \tag{17}$$

$$(\nabla\times R^a)^\mu - f^a_{bc}(A^b\times R^c) = -\frac{1}{c^2}\frac{\partial S^{a\mu}}{\partial t} + -g^{ij}T_i^{ak}\eta_k^\alpha D_\nu\eta_j^\beta C^{\mu\nu}_{\alpha\beta}/l^2, \tag{18}$$

where

$$S^a = \dot{A}^a,\ R^a = \nabla\times A^a, \tag{19}$$

and c is the phase velocity of the spatiotemporal variation of the field brought into the formalism as $\partial^\mu = (\frac{1}{c}\frac{\partial}{\partial t}, -\vec{\nabla})$ [13].

After summation over the group index a, the field equations can be put in the following form [5]:

$$\nabla\cdot\vec{v} = j^0 \tag{20}$$

$$\nabla\times\vec{\omega} = -\frac{1}{c^2}\frac{\partial\vec{v}}{\partial t} - \vec{j}, \tag{21}$$

where $j^0 = g^{ij}\eta_i^\alpha\dot{\eta}_{j\alpha}/l^2$, $\vec{j}^{\,\mu} = g^{ij}\eta_i^\alpha(D_\nu\eta_j^\beta)C^{\mu\nu}_{\alpha\beta}/l^2$, and from Eq. (19), $\vec{v}$ and $\vec{\omega}$ are related to each other as

$$\nabla\times\vec{v} = \frac{\partial\vec{\omega}}{\partial t}. \tag{22}$$

Dynamics in Plasticity

Analysis of Eq. (21) allows us to interpret $1/c^2$ on the right-hand side as representing the product of mass and shear modulus per unit volume, $1/c^2 = \varepsilon\mu$ where ε is the density and $1/\mu$ is the shear modulus [11]. Rearrangement of the terms with this expression of $1/c^2$ turns Eq. (21) to the following form [11]:

$$\varepsilon\frac{\partial\vec{v}}{\partial t} = -\frac{1}{\mu}(\nabla\times\vec{\omega}) - \frac{\vec{j}}{\mu}. \tag{23}$$

Eq. (23) can be interpreted as the equation of motion governing a unit volume of the medium, hence the constitutive relation for plasticity. Here the left-hand side of Eq.

(23) represents the external force on the unit volume, and the first and second terms on the right-hand side represent, respectively, a recovery force and a fictitious force representing the energy dissipative nature of plastic deformation. Substitution of Eq. (22) into Eq. (21) leads to a wave equation [9]. The recovery force is responsible for the oscillatory character of the wave and the energy dissipative force is for the decaying character [11].

Defining a quantity ρ as $\rho = \varepsilon\, j^0$, we can rewrite Eq. (20) as

$$\nabla \cdot \vec{v} = \frac{\rho}{\varepsilon}. \tag{24}$$

$\rho = \varepsilon(\nabla \cdot \vec{v})$ can be interpreted as the divergence in momentum associated with strain concentration $\nabla \cdot \vec{v}$. Application of divergence to both-hand side of Eq. (23) leads to an equation of continuity $\varepsilon(\partial \nabla \cdot \vec{v} / \partial t) = -(\nabla \cdot \vec{j}) / \mu$. With Eq. (24), this allows us to put $\vec{j} / \mu$ in terms of a drift velocity $\vec{W}_d$ as

$$\vec{j} / \mu = \partial / \partial t(\varepsilon \nabla \cdot \vec{v}) = \partial \rho / \partial t = \rho \vec{W}_d. \tag{25}$$

Eq. (25) indicates that the temporal change in the momentum divergence is caused only by the differential energy-dissipative-force at the boundaries [11].

Plastic Deformation and Fracture Criteria

In accordance with the gauge theoretical approach discussed above, the criteria for plastic deformation and fracture can be given as follows [14]:

$$\nabla \times \vec{\omega} \neq 0 \text{ (plastic deformation criterion)}, \tag{26}$$

$$\nabla \times \vec{\omega} = 0, \quad \vec{j} \neq 0 \text{ (fracture criterion)}. \tag{27}$$

We can understand the plastic deformation criterion by considering that in the plastic regime the transformation matrix U is local, hence the rotation $\vec{\omega}$ is coordinate-dependent making $\nabla \times \vec{\omega} \neq 0$. In the elastic regime, $\vec{\omega}$ represents rigid-body rotation, hence $\nabla \times \vec{\omega} = 0$. The fracture criterion represents that the material loses its capability of exerting the recovery force [Eq. (23)] leading to $\nabla \times \vec{\omega} = 0$. The condition $\vec{j} \neq 0$ indicates that the mechanical energy stored in the material is dissipated via $\vec{j}$ [11].

EXPERIMENTAL INVESTIGATION

Electronic Speckle-pattern Interferometry (ESPI)

Figure 3 illustrates a typical setup of in-plane sensitive ESPI [10]. In short, the light beam originating from the same laser source is split into two paths by a beam splitter,

forming the right and left interferometric arms. The light beam of each arm is reflected on the object surface, forming a number of dark and bright spots known as speckles. Consequently, on the image plane of the CCD (charge coupled device) camera the two speckle fields formed by the respective arms are superposed. Since both speckle fields result from coherent lights, the two speckle fields interfere on the image plane. The superposed speckle field is called the specklegram, whose intensity can be expressed as $I = A_1^{\,2} + A_2^{\,2} + 2A_1A_2\cos(\theta_1 - \theta_2)$ where A_1 and A_2 are the amplitude, and θ_1 and θ_2 are the phase of the right and left arm. When a certain point of the object displaces, say to the right in Figure 3, the optical path length along the right arm decreases and the optical path lengths along the left arm increases. If we subtract a specklegram corresponding to one displacement from another corresponding to another displacement, the resultant intensity profile can be given as follows:

$$\Delta I(x, y) = 2A_1A_2\sin(\theta_1 - \theta_2)\sin(\phi/2). \tag{28}$$

When the object deforms, the in-plane displacement hence the intensity profile represented by Eq. (28) becomes a function of x and y, and the corresponding image forms bright and dark fringes (Figure 4). These fringe patterns are called interferograms.

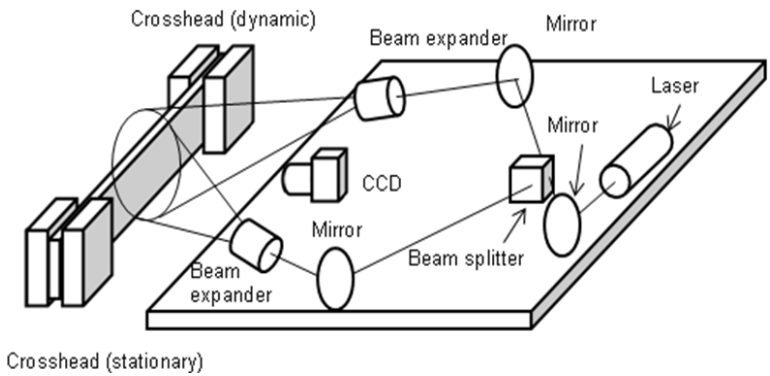

FIGURE 3. Typical experimental arrangement with an ESPI setup for in-plane deformation analysis.

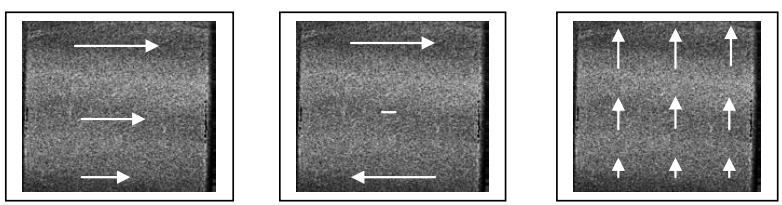

FIGURE 4. Sample interferograms with a horizontally sensitive ESPI setup (left two images) and a vertically sensitive ESPI setup (right image). Arrows represent displacement.

Fracture Prediction

By approximating the dark fringes observed in a two-dimensional fringe pattern resulting from an ESPI setup (cf. Figure 3) with second order polynomials, we can express the corresponding displacement as follows:

$$u(x,y) = a_2x^2 + a_1x + b_2y^2 + b_1y = mu_0 \tag{29}$$

$$v(x,y) = c_2x^2 + c_1x + d_2y^2 + d_1y = nv_0, \tag{30}$$

where u and v denote the horizontal and vertical displacement, respectively, m and n are integers, and u_0 and v_0 represent the unit displacement corresponding to the phase change of $\phi = 2\pi$ in Eq. (28).

With these polynomial approximations, we can express the plastic and fracture criteria as follows.

Elastic condition: The elasticity is characterized as coordinate-independent distortion matrix parameters. The first order derivatives of displacement are constant. This means that in eqs. (29) and (30) the coefficients for the second-order terms are all zero. In terms of the fringe pattern, the dark fringes are equally-spaced straight lines. If this condition is true, the deformation is elastic.

Plastic condition: If the elastic condition is not true, the deformation is plastic. It follows that if the dark fringes are curved or not equally spaced, the fringe pattern represents plastic deformation.

Fracture condition: With the polynomial expressions (29) and (30), we can rewrite the fracture condition (27) as follows:

$$(rot\ \vec{\omega})_x = \frac{\partial \omega_z}{\partial y} = \frac{\partial^2 v}{\partial x \partial y} - \frac{\partial^2 u}{\partial y^2} = -2b_2y = 0, \quad i.e., \quad b_2 = 0 \tag{31}$$

$$(rot\ \vec{\omega})_y = -\frac{\partial \omega_z}{\partial x} = -(\frac{\partial^2 v}{\partial x^2} - \frac{\partial^2 u}{\partial x \partial y}) = -2c_2x = 0, \quad i.e., \quad c_2 = 0 \tag{32}$$

$$\frac{\vec{j}}{\mu} = \varepsilon(\frac{\partial u}{\partial x} + \frac{\partial v}{\partial y})\vec{W}_d = \varepsilon(2a_2x + a_1 + 2d_2y + d_1)\vec{W}_d \neq 0, \tag{33}$$

where Eq. (25) is used in Eq. (33). Eq. (31) indicates that under the fracture condition the horizontally sensitive fringe $u(x,y)$ does not have second order dependence on y while it can have second order dependence on x. Similarly, Eq. (32) indicates that the vertically sensitive fringes $v(x,y)$ does not have second order dependence on x but can have second order dependence on y. Table 1 lists all the possible combinations for the coefficients of the horizontally sensitive fringes to satisfy condition Eq. (31).

TABLE 1. Possible combinations of coefficient of $u(x, y)$ to satisfy condition (31)

Case	1	2	3	4	5	6	7	8
a_2	$\neq 0$	$\neq 0$	$\neq 0$	$\neq 0$	$= 0$	$= 0$	$= 0$	$= 0$
a_1	$\neq 0$	$\neq 0$	$= 0$	$= 0$	$\neq 0$	$= 0$	$\neq 0$	$= 0$
b_1	$\neq 0$	$= 0$	$\neq 0$	$= 0$	$= 0$	$\neq 0$	$\neq 0$	$= 0$

Table 2 shows the shape and expression of the dark fringes for each combination in Table 1. Table 3 shows the corresponding cases for the vertically sensitive fringes.

TABLE 2. Equation and shape of horizontally sensitive fringes $u(x, y)$ under fracture condition

Case	Equation and Shape of Fringes
1	$a_2x^2 + a_1x + b_1y = mu_0$, vertical parabolas
2	$a_2x^2 + a_1x = mu_0$, compressed, vertical straight lines
3	$a_2x^2 + b_1y = mu_0$, vertical parabolas
4	$a_2x^2 = mu_0$, compressed, vertical straight lines
5	$a_1x = mu_0$, equally-spaced, vertical straight lines
6	$b_1y = mu_0$, equally-spaced, horizontal straight lines
7	$a_1x + b_1y = mu_0$, equally-spaced, slant straight lines
8	Trivial

TABLE 3. Equation and shape of vertically sensitive fringes $v(x, y)$ under fracture condition

Case	Equation and Shape of Fringes
1’	$d_2y^2 + d_1y + c_1x = nv_0$, horizontal parabolas
2’	$d_2y^2 + d_1y = nv_0$, compressed, horizontal straight lines
3’	$d_2y^2 + c_1x = nv_0$, horizontal parabolas
4’	$d_2y^2 = nv_0$, compressed, horizontal straight lines
5’	$d_1y = nv_0$, equally-spaced, horizontal straight lines
6’	$c_1x = nv_0$, equally-spaced, vertical straight lines
7’	$d_1x + c_1y = nv_0$, equally-spaced, slant straight lines
8’	Trivial

With the above argument in mind, we can examine fringe patterns observed in experiments. Figure 5 shows interferograms resulting from an experiment in which we applied a tensile load to a 20 mm (wide) x 100 mm (long) x 0.4 mm (thick) tin specimen at a constant pulling rate of 4 μm/s until it fractured. We used an experimental arrangement similar to Figure 3. To observe horizontal and vertical displacement simultaneously, we arranged an additional interferometer sensitive to vertical displacement on the rear side of the specimen, and captured the specklegrams of both surfaces simultaneously with the same CCD camera by arranging the imaging mirrors appropriately. We captured the specklegrams continuously at the maximum frame rate of 30 frames/s, and subtracted a specklegram captured at a later time step. In Figure 5, the images in the upper and lower rows are representative horizontally and

vertically sensitive fringes. The pair of the images in the same column are the fringes formed from the specklegrams taken at the same time steps. The lower plot in Fig. 5 is the corresponding loading characteristics where (a) - (e) indicate the points when the fringe patterns labeled (a) - (e) are formed.

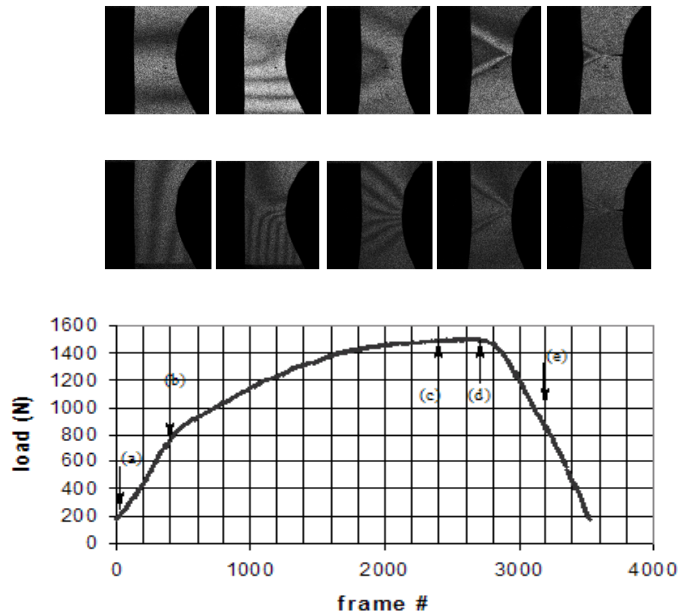

FIGURE 5. Vertically and horizontally sensitive fringe patterns (top) and corresponding loading characteristics (bottom). The numbers under the images are frame numbers. "V" and "H" denote "vertically "and "horizontally" sensitive fringes.

The following observations support the above argument.

Fringes in (a): Being all straight lines and equally spaced, these fringes represent elastic deformation. The loading characteristic supports this observation indicating that the stress-strain relationship is in the linear range when these fringes are formed.

Fringes in (b) - (c): Fringes (b) correspond to the point where the linear stress-strain relationship is about to end. Note that near the vertical center of the images, the horizontally/vertically sensitive fringes show horizontal/vertical parabolas. From the above argument, this indicates that the material deforms plastically but has not reached the fracturing stage. The same tendency (the horizontally/vertically sensitive fringes show horizontal/vertical parabolas) continues till point (c).

Fringes in (d): At this point, the horizontally/vertically sensitive fringes lose the horizontal/vertical curvatures, becoming straight lines. These satisfy the fracture conditions 7 and 7'. Short after this point, the loading curve begins to decrease,

supporting this observation. It is interesting to note that the fracture condition is satisfied in the horizontally and vertically sensitive fringes at the same time.

Fringes in (e): These fringes are typically observed in the last stage of deformation where the load decreases monotonically. Normally, the horizontally and vertically sensitive fringes show similar slant straight lines that move with the crack tip until the specimen completely fractures. Apparently, condition (33) is satisfied.

SUMMARY

Deformation of solid-state materials has been formulated based on the local linear transformation and the associated gauge invariance. Dynamics of plastic deformation and the constitutive equation has been derived. Plastic deformation and fracture criteria resulting from the present formalism have been validated by optical interferometric displacement analysis conducted for a tensile experiment. Being capable of describing all stages of deformation on the same theoretical basis, the present formalism is applicable to various engineering problems.

ACKNOWLEDGMENTS

The present work has been in part supported by the Southeastern Louisiana University Alumni Association and Faculty Development Grants. Experimental supports by Robert L. Rourks and discussion with Malik Rakhmanov are appreciated.

REFERENCES

1. L. D. Landau and E. M. Lifshitz, *Theory of Elasticity, 3rd edn., Course of Theoretical Physics, Vol. 7*, Butterworth-Heinmann, Oxford, 1986.
2. W. Sylwestrowicz and E. O. Hall, Proc. Phys. Soc. London, Sect. B **64**, 495-502.
3. J. M. Barson and S. T. Rolfe, *Fracture and Fatigue Control in Structures*, 3rd edn., ASTM, Philadelphia, 1999.
4. V. E. Panin (ed.), *Physical Mesomechanics of Heterogeneous Media and Computer-Aided Design of Materials, vol. 1*, Cambridge International Science, Cambridge, 1998.
5. V. E. Panin et al., *Sov. Phys. J.* **30**, 24-38 (1987).
6. Wikipedia, "Gauge invariance," `http://en.wikipedia.org/wiki/Gauge_theory`, accessed September 8, 2009.
7. I. J. R. Aitchson and A. J. G. Hey, *Gauge theories in particle physics*, IOP Publishing, Bristol and Philadelphia, 1989.
8. J. Salençon, *Handbook of continuum mechanics*, p. 12, Springer-Verlag, Berlin, 2001.
9. S. Yoshida et al, *Phys. Lett. A* **251**, 54-60 (1999).
10. R. S. Sirohi (ed.), *Speckle Metrology*, Marcel Dekker, Inc., New York, 1993.
11. S. Yoshida, *Physical Mesomechanics*, **11**, 140-146 (2008).
12. S. Yoshida, in *Proc. NANOMEC06, Nov. 19-23, 2006, Bari, Italy*, 2006.
13. Wikipedia, "Electromagnetic tensor," `http://en.wikipedia.org/wiki/Electromagnetic_tensor`, accessed September 8, 2009.
14. S. Yoshida, *Phys.. Lett. A* **270**, 320-325 (2000).